SCIENTIFIC ARTICLE

3D models of nonunion fractures in long bones as education tools

Criação e impressão 3D de modelos de união de fraturas para o ensino de medicina veterinária

BJVM
Brazilian Journal of Veterinary Medicine

p-ISSN 0100-2430
e-ISSN 2527-2179

Katriny Elifelina Monteiro Rodrigues[1], Kleber dos Anjos Lucas[1], Andrey Luiz Lopes Cordeiro[2], Romeu Paulo Martins Silva[3], Francisco Glauco de Araújo Santos[4] & Yuri Karaccas de Carvalho[4]*

[1]Undergraduate in Veterinary Medicine, Centro de Ciência Biológicas e da Natureza (CCBN), Universidade Federal do Acre (UFAC), Rio Branco, AC, Brasil
[2]Veterinarian, MSc. Programa de Pós-Graduação Sanidade e Produção Animal Sustentável na Amazônia Ocidental (PPGESPA), CCBN, UFAC, Rio Branco, AC, Brasil
[3]Physical educator, DSc., Departamento de Biotecnologia, Universidade Federal do Catalão (UFCAT), Catalão, GO, Brasil
[4]Veterinarian, DSc., CCBN, UFAC, Rio Branco, AC, Brasil

Abstract

The appearance of fracture complications can present itself as a difficult scenario in a veterinarian's practice, and it can be difficult to diagnose and have a poor prognosis. The recognition of the different types of nonunion fractures can enable quick guidance on the best way to act, thus reducing the cost of treatment and the patient's suffering. The objective of this study was to create 3D models of nonunion fractures in long bones (3D NUFs). The study was carried out in three stages: 1) creating biscuit models from representations of nonunion fractures; 2) scanning the biscuit models of nonunion fractures and 3D modeling; and 3) printing and finishing the 3D models of nonunion fractures (hereafter, 3D NUFs). The creation of biscuit prototypes and the respective digitalization were decisive in producing 3D NUF's, which reproduced the main characteristics of each type of nonunion fracture classification described in the literature. It took 31.1 hours to create and print all 3D NUFs using 95.66 grams of filament (ABS) for a total cost of $3.73. The creation of 3D NUFs from the biscuit dough presented a new way of obtaining didactic models for the teaching of veterinary medicine. The 3D NUFs represent the different forms of low-cost manifestations that characterize this disease, which can be used as a possible teaching-learning tool for veterinary education.

Keywords: anatomy, orthopedics, veterinary education, 3D printing.

Resumo

O surgimento de complicações de fraturas pode se apresentar como um cenário difícil na prática do médico veterinário e pode ser difícil de diagnosticar e ter um prognóstico ruim. O reconhecimento dos diferentes tipos de não união de fraturas pode permitir orientação rápida sobre a melhor maneira de agir, reduzindo o custo do tratamento e o sofrimento do paciente. O objetivo deste estudo foi criar modelos 3D de não união de fraturas em ossos longos (3D NUF). O estudo foi em três etapas: 1. Criação dos modelos de *biscuit* a partir de representações de não união de fraturas; 2. Digitalização dos modelos de *biscuit* de fraturas sem união e modelagem 3D; 3. Impressão e acabamento de modelos 3D de fraturas sem união (3D NUF). A confecção de protótipos em biscuit e a respectiva digitalização foram decisivas para a produção de NUF 3D. O NUF 3D reproduziu as principais características de cada tipo de classificação de não união de fratura descrita na literatura. Foram necessárias 31,1 horas para criar e imprimir todo o 3D NUF, usando 95,66 gramas de filamento (ABS) a um custo total de US $ 3,73. A criação do 3D NUF a partir da massa de *biscuit* apresentou uma nova maneira de obter modelos didáticos para o Ensino de Medicina Veterinária. O NUF 3D representou as diferentes formas de manifestação que caracterizam esta doença a baixo custo, que podem ser utilizadas no ensino de assuntos como anatomia e cirurgia.

Palavras-chave: anatomia, ortopedia, material de ensino, impressão 3D.

How to cite: Rodrigues, K. E. M., Lucas, K. A., Cordeiro, A. L. L., Silva, R. P. M., Santos, F. G. A., & Carvalho, Y. K. (2021). 3D models of nonunion fractures in long bones as education tools. *Brazilian Journal of Veterinary Medicine*, *43*, e114820. https://doi.org/10.29374/2527-2179.bjvm114820

Received: July 28, 2020.
Accepted: October 23, 2020.

***Correspondence**
Yuri Karaccas de Carvalho
Centro de Ciências Biológicas e da Natureza,
Universidade Federal do Acre – UFAC
Rodovia BR 364, Km 04, Distrito Industrial
CEP 69920-900 - Rio Branco (AC), Brasil
E-mail: ykaracas@yahoo.com.br

Introduction

The reconstruction of orthopedic fractures in dogs—especially those involving long bones—is part of a veterinarian's daily activities. Long bone fractures account for 7.33% of all surgical cases, and their repair is extremely important in enabling an affected limb to return quickly to its function (Jain et al., 2018; Keosengthong et al., 2019; Kushwaha et al., 2011). The healing process is continuous, however, with variable completion times. The influencing factors are age, species, breed, bone involvement, fracture level, and associated tissue damage (Denny & Butterworth, 2006). The fracture may not join, which is characterized by the cessation of the entire repair process. This complication usually results from an iatrogenic failure (Frölke & Patka, 2007; Polyzois et al., 2006).

There are still no reports of the incidence rates of nonunion fractures in veterinary medicine (Massie et al., 2017). In humans, the rates of this complication can reach 10% of the relevant cases (Pugh & Rozbruch, 2018). Nonunion fractures are classified into seven types: hypertrophic or elephant's foot, slightly hypertrophic or horse's hoof, hypotrophic, atrophic, torsion wedge, comminuted, and bone gap (Denny & Butterworth, 2006; Weber & Cech, 1976).

Veterinary medicine students learn the complications of bone fractures mainly through books, medical images, and clinical cases (Smith et al., 2018). Furthermore, it is believed that the use of 3D didactic models to explain orthopedics can be an excellent tool for improving the teaching of veterinary medicine (Lima et al., 2019; Nunez et al., 2020).

The use of 3D printing is already a reality in different areas of veterinary medicine, such as orthopedics (Dismukes et al., 2008), diagnostic imaging (Preece et al., 2013), and especially, as a 3D didactic model creation tool for teaching (Nibblett et al., 2017; Thomas et al., 2016). It is an excellent source of high-quality materials for veterinary medicine instruction (Lima et al., 2019; Neves et al., 2020; Nunez et al., 2020).

The objective of this study was to develop 3D models that represent the classifications of nonunion fractures (3D NUFs) in long bones.

Materials and methods

The study was developed at the 3D Educational Technologies Laboratory of the Federal University of Acre; it took place in three stages: 1) creating biscuit models from representations of nonunion fractures; 2) scanning the biscuit models of nonunion fractures and 3D modeling; and 3) printing and finishing the 3D models of nonunion fractures (3D NUFs) (Figure 1). The experiment protocol did not involve the use of animals or a submission to the Animal Research Ethics Committee.

Creation of biscuit models from representations of nonunion fractures

The first models of nonunion fractures were made from biscuit dough. Also known as cold porcelain, a biscuit is a pastry made from white glue, cornstarch, lemon, vinegar, and petroleum jelly. Currently, it is a widely used in the preparation of various types of handicrafts.

The representative biscuit models of nonunion fractures were made based on the classification proposed by Weber and Cech (1976) and distributed in two groups: vascular or viable and nonvascular or nonviable (Denny & Butterworth, 2006) (Table 1).

Scanning the biscuit models of nonunion fractures and 3D modeling

The 3D NUF creation process consisted of digitizing the biscuit models and perfecting them using software and, later, 3D printing. The models were digitized using the 3D scanner, Model EinScan-SP (Shining 3D®, Zhejiang, China), with the aid of the EinScan-SP Version 2.6.0.8 software, which has a scanning accuracy of ≤ 0, 05 mm and 0.17–0.2 mm capture size.

The digital files obtained were saved in stereolithography format (*.stl*), and stored in the database. Subsequently, they were transferred to the Autodesk Meshmixer® 3D image manipulation software, version 3.1 (Autodesk© Inc., California, United States). The software facilitated the use of tools that corrected and improved the images generated by eliminating uneven surfaces.

Printing and finishing 3D fracture non-joining models

The 3D NUFs were printed on the GTMax 3D Core A1V2® equipment (GtMax Electronics Technology Ltd., Sao Paulo, Brazil) that uses fused deposition modeling (FDM) technology and thermoplastic material, type ABS (i.e., acrylonitrile butadiene styrene). The print settings were as follows: 1) high quality; 2) 99% internal filling, and 3) Z layer thickness of 0.15 mm.

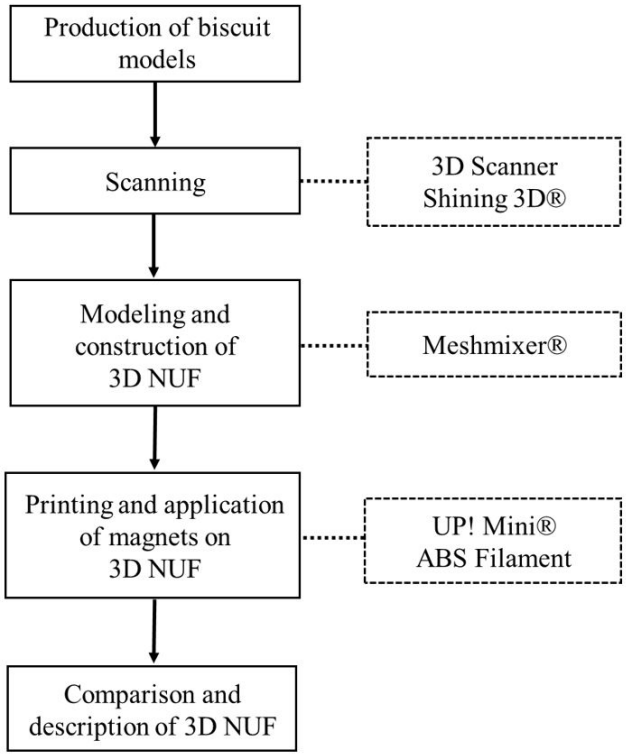

Figure 1. Flowchart of creation of 3D models of fracture non-union (3D NUF).

Table 1. Classification of types of fracture non-union.

	Types	Features
Vascular or viable	Hypertrophic or Elephant's foot	The formation of a large bone callus occurs, which gives it the appearance of an "elephant's foot"
	Slightly hypertrophic or Horse's hoof	The formation of the bony callus is not as exacerbated as in the hypertrophic one
	Hypotrophic	The fracture ends are rounded, with little or no bone callus formation
	Comminuted	It has one or more intermediate bone fragments
Non-vascular or non-viable	Atrophic	It has a space between the extremities and the medullary channels are sealed by scar tissue
	Torsion wedge	Presence of an intermediate bone fragment that prevents the blood supply
	Bone gap	Loss of a bone fragment occurs so that the fracture cannot join

Adapted from Denny & Butterworth (2006), Weber & Cech (1976).

A total of seven 3D NUFs were printed; each model represented a different type of nonunion fracture classification. After printing, manual finishes were applied to each model (e.g., sanding and painting with oil-based paint). During the entire process of constructing the 3D NUFs, the creation times for the biscuit and 3D models, printing times, quantity of material used, and cost of printing were recorded.

The time involved in creating the biscuit models corresponded to the dough handling, modeling, and painting process. The time involved in creating the 3D models corresponded to the process of digitizing and processing the images in the software to obtain the files for printing. The printing time corresponded to the period necessary to build the 3D NUFs. The amount of material used corresponded to the total mass of the filament employed to build the support structure and create each model. The printing cost corresponded to the production value of each model and included the cost of 3D filament, electricity, and depreciation of the equipment used. Values referring to the initial investment for the acquisition of equipment (scanner and 3D printer) were excluded.

Results

The 3D NUFs were similar to the illustrations and biscuit models produced. The time for creation, printing, quantity of material used, and final cost of producing the models varied according to the complexity and size of the model. The 3D model NFU-bone gap took the longest to create in biscuit dough. The 3D NFU-torsion wedge required the longest printing time (Table 2).

The biscuit models and 3D NUF models represented the classifications of the nonunion of vascular or viable fractures (hypertrophic, slightly hypertrophic, and hypotrophic) and the nonunion of avascular or nonviable fractures (comminuted, atrophic, torsion wedge, and bone gap).

The 3D NUF-hypertrophic model (Figure 2.A2) consisted of two portions representing proximal and distal fragments of the bone interposed by the bone callus. In this model, we highlighted the bone callus as a mass of great dimensions, both in width and height, and with its lateral edges transcending the two parts of the model.

The 3D NUF-slightly hypertrophic model (Figure 2.B2) was also represented by two portions as two proximal and distal bone fragments mediated by a mass representing the bone callus. In this model, the bone callus representation had smaller dimensions (width and height) than those represented by the 3D NUF-hypertrophic model.

The 3D NUF-hypotrophic model (Figure 2.C2) was illustrated by two portions representing the proximal and distal bone fragments with their slightly rounded edges. The connection of the bone fragments was given by the representation of a short and narrow bone callus and smaller lateral edges than the other portions of the model.

Table 2. Biscuit creation time (Bct), 3D NUF creation time (3D NUF ct), 3D NUF printing time (3D NUF pt), Amount of material used for 3D NUF (Amu 3D NUF) and Cost of 3D NUF.

3D NFU	Bct (h)	3D NUF ct (h)	3D NUF pt (h)	Amu 3D NUF (g)	Cost (US$)
Hypertrophic	0.75	0.66	2.46	14.21	0.56
Slightly hypertrophic	1.32	0.58	2.33	10.99	0.42
Hypotrophic	1.42	0.83	2.4	12.63	0.49
Comminuted	2.25	0.58	2.43	12.66	0.5
Atrophic	1.15	0.75	2.42	10.86	0.42
Torsion wedge	0.68	0.63	2.6	10.95	0.42
Bone gap	2.35	1	1.65	10.73	0.41
TOTAL	9.82	5.03	16.27	95.66	3.73

(h) – Hours; (g) – Grams; (US$) – Dollar. Classification of types of fracture non-union after Denny & Butterworth (2006), Weber & Cech (1976).

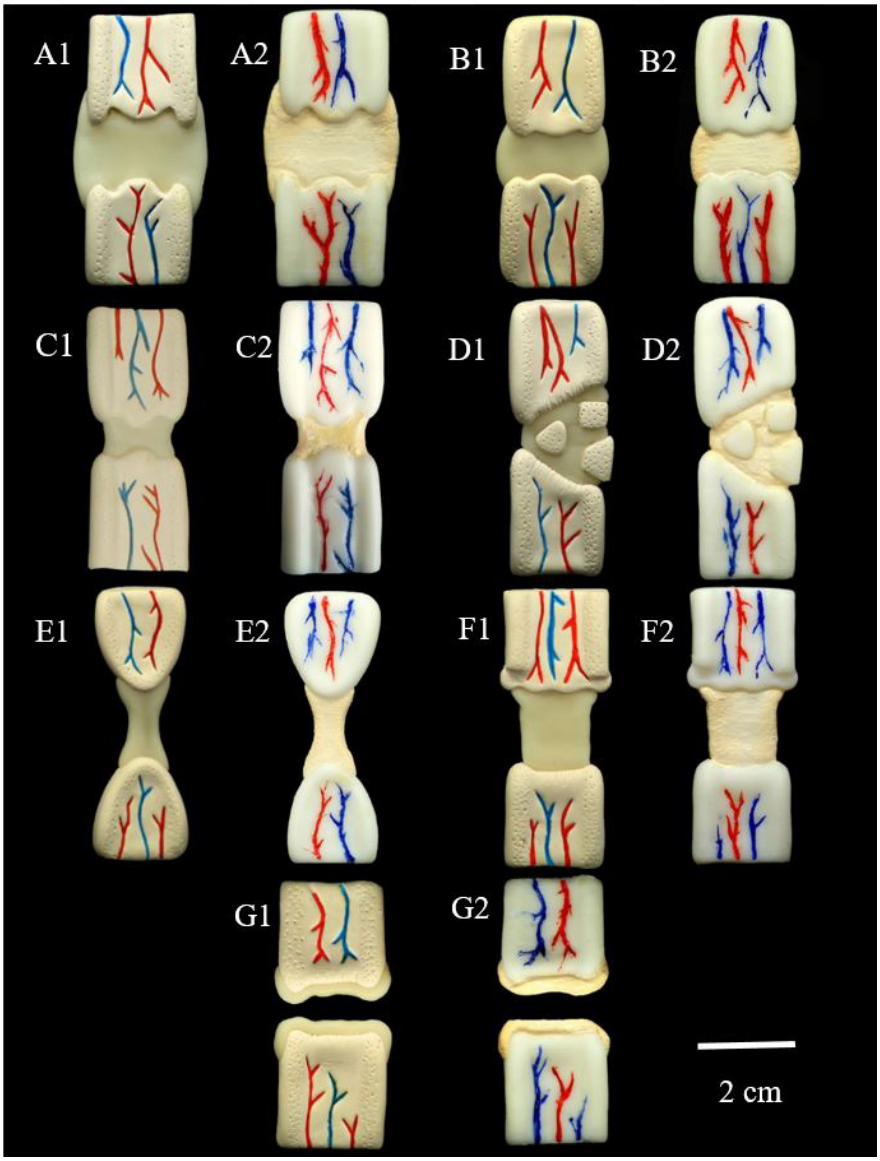

Figure 2. Representation of the classification of non-union of fractures. (A) Hypertrophic or Elephant's foot; (B) Slightly hypertrophic or Horse's roof; (C) Hypotrophic; (D) Comminuted; (E) Atrophic; (F) Torsion wedge; (G) Bone gap; 1. *Biscuit* model of different types of fracture non-union; 2. 3D models of fracture non-union. Classification of types of fracture non-union after Denny & Butterworth (2006), Weber & Cech (1976).

The 3D NUF-comminuted model Figure 2.D2) was demonstrated by five portions representing two bone fragments (proximal and distal) in a bevel shape, intermediated by three small, scattered bone fragments.

The 3D NUF-atrophic model (Figure 2.E2) was formed by two portions representing two bone fragments (proximal and distal) in a triangular shape and with a rounded apex. The connection between the two portions was given by a long and narrow mass. In terms of shape, the model resembles an hourglass.

The 3D NUF-torsion wedge model (Figure 2.F2) was given two portions representing the two main bone fragments (proximal and distal). The connection was illustrated by a mass with smaller side edges than the other parts of the model.

The 3D NUF-bone gap model (Figure 2.G2) was illustrated by two portions representing two bone fragments (proximal and distal). The model showed the complete lack of bone union (i.e., no callus formation and the ends remain separate).

Discussion

The creation of a 3D NUF model originated from the need to develop materials for teaching about nonunion fractures, since this complication has been approached during classes mainly through diagrams and figures. This disease is difficult to diagnose and has low casuistry, making it difficult to demonstrate in practice (Mills et al., 2017; Zimmermann et al., 2007). The use of 3D didactic models during classes helps students assimilate knowledge; further, it increases their interest and enthusiasm and allows learning to occur more effectively (Li et al., 2015; Vranicar et al., 2008).

A 3D NUF model enables the 3D representation of the different forms of nonunion fractures that may occur, which can increase students' visual and spatial understanding of the disease. In this sense, when reproducing a 3D horse foot to demonstrate spatial relationships, the authors concluded that physical models have a significant advantage over other learning resources (Preece et al., 2013).

The choice regarding the representation of the classifications of nonunion fractures by means of a biscuit model to perform 3D scanning was due to the absence of preexisting models. Furthermore, there is difficulty in accessing medical images (e.g., computed tomography) that exemplify this disease (Zimmermann et al., 2007). The use of biscuit dough for making didactic models has already been described as part of the methodology of teaching entomology, biochemistry, embryology, and genetics, which is often used for ease of production, cost, malleability, and handling of the dough (Matos et al., 2009; Souza & Alves, 2016; Zierer, 2017). The use of biscuit dough for the purpose of producing didactic models on a scale is limited since it is an artisanal material and the result depends mainly on the skill of the handler (Souza & Alves, 2016). In this sense, the use of biscuit dough for prototypes of teaching models is recommended for use as an intermediate step in the process of creating 3D models from scans.

The time involved in creating the biscuit models was approximately 10 hours. However, after making the pieces, a drying period of 24 hours was necessary. This process clearly takes time, considering the drying period needed for the finish. The digitization stage was extremely important for the development of the study since it enabled the generation of high-quality images necessary for the development of 3D NUFs. These images allowed the main points of the representations of the different models of nonunion fractures to be preserved. These findings corroborate those of Li et al. (2018), who produced three 3D models (i.e., rib, femur, and cervical vertebra of a bovine) and Lima et al. (2019), who produced a 3D canine jaw. The studies mentioned describe and emphasize how the precision and quality of scanning influences the process of creating anatomical models.

The creation time for the 3D NUFs was 5.03 hours and basically represented the digitization of each of the seven biscuit models. The manipulation of the images generated by the 3D scanner was restricted to formatting details at the ends of the models, such as removing the adhesive tape that affixed the biscuit model to the scanner table.

Details were superficial and of limited quantity in the aforementioned 3D NUF The 3D NUF model for having superficial details and in little quantity (e.g., the representation of vessels and morphology of the fractured region), but had a positive impact on the scanning and post-production time of the generated file. These findings corroborate the study of Thawani et al. (2016), who stated that producing a model of arteriovenous malformation requires 10 hours; the greater the complexity of the model, the greater the scanning time.

The total time involved in printing the 3D NUF model (approximately 16 hours) was considered high compared to the time involved in printing a 3D model of a canine skull (7 hours) (Hespel et al., 2014). However, it is worth noting that this amount of time can be justified by the settings used during our study (internal filling of the model, layer thickness, temperature, and support structures), which directly influence the precision and print quality of the created models (Chung et al., 2018; Reis et al., 2019).

The production cost for the 3D NUF was relatively low when the initial investment in scanning and printing equipment was excluded. In this study, 95.66 g of filament were used at a cost that did not exceed US $3.73. The parameters used to calculate the cost of production were also adopted in other studies; after the initial investment in scanning and printing equipment, the

cost of producing 3D models was low (Lima et al., 2019; Nunez et al., 2020). Furthermore, costs may become even lower when the highest possible resolution of our 3D printer is used, as it directly impacts the amount of material used for printing.

There were small differences between the 3D NUF models and the illustrations that depict the classifications of nonunion fractures in long bones recommended by Weber & Cech (1976). However, the morphology and identification of the main portions that identify the different types of nonunion fractures were maintained, with no bias in identifying the type of nonunion fracture. It is worth noting that these small differences represent a limitation of the technique for obtaining biscuit prototypes for scanning because of the subjectivism and ability of those who produce models representing the different types of nonunion fractures (Souza & Alves, 2016).

A 3D NUF model can also promote the relevant database so that any interested person or educational institution can have access to it. These findings corroborate those of other studies that shared their creations—such as a 3D model of an ear canal—on the Thingiverse© digital platform (Nibblett et al., 2017).

Conclusions

The creation of 3D NUF models from biscuit dough is a new way of obtaining didactic models for teaching veterinary medicine. The 3D NUF models representing the different manifestations that characterize this disease incur a low cost, and they can be used for teaching such subjects as anatomy and surgery.

Acknowledgements

Contributed to this work the entire team of the 3D Educational Technologies Laboratory of the Federal University of Acre.

Ethics statement

The experiment protocol was approved by the Animal Research Ethics Committee of the Federal University of Acre (CEUA-UFAC), protocol number 59/16.

Financial support

This study was financed (Grant term n.26/2018 - PPP- FAPAC/CNPq - Brazil; Grant term n.33/2018 - PPSUS- FAPAC- Brazil).

Conflict of interests

KEMR, KAL, ALLC, RPMS, FGAS and YKC - No conflict of interest.

Authors' contributions

KEMR and KAL - Acquisition and Technical procedures. ALLC - Acquisition and analysis and interpretation of data. RPMS - Manuscript writing, critical revision, final approval. FGAS and YKC - Analysis and interpretation of data, manuscript writing, and final approval.

Availability of complementary results

None.

The study was carried out at Universidade Federal do Acre - UFAC, Rio Branco, AC, Brasil.

References

Chung, M., Radacsi, N., Robert, C., Mccarthy, E. D., Callanan, A., Conlisk, N., Hoskins, P. R. & Koutsos, V. (2018) On the optimization of low-cost FDM 3D printers for accurate replication of patient-specific abdominal aortic aneurysm geometry. *3D Printing in Medicine*, *4*(1), 1-10. http://dx.doi.org/10.1186/s41205-017-0023-2 PMID: 29782613

Denny, H. R., & Butterworth, S. J. (2006). Complicações das fraturas. In S. Butterworth & H. Denny (Eds.), *Cirurgia Ortopédica em Cães e Gatos* (4a ed., pp. 103-118). São Paulo: Roca.

Dismukes, D. I., Fox, D. B., Tomlinson, L. J., & Essman, S. C. (2008). Use of radiographic measures and three-dimensional computed tomographic imaging in surgical correction of an antebrachial deformity in a dog. *Journal of the American Veterinary Medical Association*, *232*(1), 68-73. http://dx.doi.org/10.2460/javma.232.1.68. PMid:18167111.

Frölke, J. P., & Patka, P. (2007). Definition and classification of fracture non-unions. *International journal of the Care Injured,* 38, 19-22. http://dx.doi.org/0.1016/s0020-1383(07)80005-2.

Hespel, A. M., Wilhite, R., & Hudson, J. (2014). Invited review-applications for 3D printers in veterinary medicine. *Veterinary Radiology & Ultrasound*, *55*(4), 347-358. http://dx.doi.org/10.1111/vru.12176. PMid:24889058.

Jain, R., Shukla, B. P., Nema, S., Supriya, S., Daljeet, C., & Karmore, S. K. (2018). Incidence of fracture in dog: a retrospective study. *Veterinary Practitioner,* 19, 63-65. http://www.vetpract.in/Archives/June--2018/incidence-of-fracture-in-dog-a-retrospective-study/

Keosengthong, A., Kampa, N., Jitpean, S., Seesupa, S., Kunkitti, P., & Hoisang, S. (2019). Incidence and classification of bone fracture in dogs and cats: a retrospective study at veterinary teaching hospital, Khon Kaen university, Thailand (2013-2016). *Veterinary Integrative Sciences, 17*(2), 127-139. https://he02.tci-thaijo.org/index.php/vis/article/view/135358

Kushwaha, R. B., Gupta, A. K., Bhadwal, M. S., Kumar, S., & Tripathi, A. K. (2011). Incidence of fractures and their management in animals: A clinical study of 77 cases. *Indian Journal of Veterinary Surgery*, *32*, 54-56.

Li, F., Liu, C., Song, X., Huan, Y., Gao, S., & Jiang, Z. (2018). Production of accurate skeletal models of domestic animals using three-dimensional scanning and printing technology. *Anatomical Sciences Education*, *11*(1), 73-80. http://dx.doi.org/10.1002/ase.1725. PMid:28914982.

Li, Z., Li, Z., Xu, R., Li, M., Li, J., Liu, Y., Sui, D., Zhang, W., & Chen, Z. (2015). Three-dimensional printing models improve understanding of spinal fracture: A randomized controlled study in China. *Scientific Reports*, *5*(1), 11570. http://dx.doi.org/10.1038/srep11570. PMid:26099838.

Lima, A. S., Machado, M., Pereira, R. C. R., & Carvalho, Y. K. (2019). Printing 3D models of canine jaw fractures for teaching undergraduate veterinary medicine. *Acta Cirurgica Brasileira*, *34*(9), e201900906. http://dx.doi.org/10.1590/s0102-865020190090000006. PMid:31826098.

Massie, A., Fuller, M., Verstraete, F., Arzi, B., & Kapatkin, A. (2017). Outcome of nonunion fractures in dogs treated with fixation compression resistant matrix, and recombinant human bone morphogenetic protein-2. *Veterinary and Comparative Orthopaedics and Traumatology: V.C.O.T*, *30*(2), 153-159. http://dx.doi.org/10.3415/VCOT-16-05-0082. PMid:28094415.

Matos, C. H. C., Oliveira, C. R. F., Santos, M. P. F., & Ferraz, C. S. (2009). Utilização de modelos didáticos no ensino de entomologia. *Revista de Biologia e Ciências da Terra*, *9*(1), 19-23.

Mills, L. A., Aitken, S. A., & Simpson, H. R. W. (2017). The risk of non-union per fracture: Current myths and revised figures from a population of over 4 million. *Acta Orthopaedica*, *88*(4), 434-439. http://dx.doi.org/10.1080/17453674.2017.1321351. PMid:28508682.

Neves, E. C., Pelizzari, C., Oliveira, R. S., Kassab, S., Lucas, K. A., & Carvalho, Y. K. (2020). 3D Anatomical model for teaching canine lumbosacral epidural anesthesia. *Acta Cirurgica Brasileira*, *35*(6):e202000608. http://dx.doi.org/10.1590/s0102-865020200060000008. PMid:32667587.

Nibblett, B. M. D., Pereira, M. M., Sithole, F., Orchard, P. A. D., & Bauman, E. B. (2017). Design and Validation of a Three-Dimensional Printed Flexible Canine Otoscopy Teaching Model. *Simulation in Healthcare: Journal of the Society for Simulation in Healthcare*, *12*(2), 91-95. http://dx.doi.org/10.1097/SIH.0000000000000227. PMid:28383365.

Nunez, R. Y. G., Albuquerque, L. K., Pereira, R. C. R., Silva, R. P. M., Peruquetti, P. F., & Carvalho, Y. K. (2020). 3D printing of canine hip dysplasia: Anatomic models and radiographs. *Arquivo Brasileiro de Medicina Veterinária e Zootecnia*, *72*(3), 769-777. http://dx.doi.org/10.1590/1678-4162-10899.

Polyzois, V. D., Papakostas, I., Stamatis, E. D., Zgonis, T., & Beris, A. E. (2006). Current concepts in delayed bone union and non-union. *Clinics in Podiatric Medicine and Surgery*, *23*(2), 445-453, viii. http://dx.doi.org/10.1016/j.cpm.2006.01.005. PMid:16903161.

Preece, D., Williams, S. B., Lam, R., & Weller, R. (2013). "Let's get physical": Advantages of a physical model over 3D computer models and textbooks in learning imaging anatomy. *Anatomical Sciences Education*, *6*(4), 216-224. http://dx.doi.org/10.1002/ase.1345. PMid:23349117.

Pugh, K. J., & Rozbruch, S. R. (2018). Nonunion and malunions. In M.D. Javad Parvizi (Ed.), *Orthopaedic knowledge Update* (12nd ed., pp. 115-130). American Academy of Orthopaedic Surgeons.

Reis, D. A. L., Gouveia, B. L. R., Junior, J. C. R. & Assis Neto, A. C. (2019). Comparative assessment of anatomical details of thoracic limb bones of a horse to that of models produced via scanning and 3D printing. *3D Printing in Medicine, 5*, 13. http://dx.doi.org/10.1186/s41205-019-0050-2. PMID: 31375944

Smith, C. F., Tollemache, N., Covill, D., & Johnston, M. (2018). Take away body parts! An investigation into the use of 3D-printed anatomical models in undergraduate anatomy education. *Anatomical Sciences Education*, *11*(1), 44-53. http://dx.doi.org/10.1002/ase.1718. PMid:28753247.

Souza, R. T. B., & Alves, M. H. (2016). Modelos didáticos com massa de *biscuit*: Inovando no ensino de ciências e biologia. *Espacios*, *37*(29), 8.

Thawani, J. P., Pisapia, J. M., Singh, N., Petrov, D., Schuster, J. M., Hurst, R. W., Zager, E. L., & Pukenas, B. A. (2016). Three-dimensional printed modeling of an arteriovenous malformation including blood flow. *World Neurosurgery*, 90, pp. 675-683.e.2. https://dx.doi.org/10.1016/j.wneu.2016.03.095.

Thomas, D. B., Hiscox, J. D., Dixon, B. J., & Potgieter, J. (2016). 3D scanning and printing skeletal tissues for anatomy education. *Journal of Anatomy*, *229*(3), 473-481. http://dx.doi.org/10.1111/joa.12484. PMid:27146106.

Vranicar, M., Gregory, W., Douglas, W. I., Di Sessa, P., & Di Sessa, T. G. (2008). The use of stereolithographic hand held models for evaluation of congenital anomalies of the great arteries. *Studies in Health Technology and Informatics*, *132*, 538-543. PMid:18391364.

Weber, B. G., & Cech, O. (1976). *Pseudarthrosis, pathology, biomechanics, therapy, results.* Hans Huber.

Zierer, M. S. (2017). The construction and application of didactic models in biochemistry teaching. *Journal of Biochemistry Education.*, *15*, 1-10.

Zimmermann, G., Muller, U., & Wentzensen, A. (2007). The value of laboratory and imaging studies in the evaluation of long-bone non-unions. *Injury*, *38*(Suppl 2), S33-S37. http://dx.doi.org/10.1016/S0020-1383(07)80007-6. PMid:17920416.